Electronic Supplementary Information

Experimental Section

Materials: All reagents used in this work are analytical grade. Cobalt nitrate hexahydrate ($Co(NO_3)_2 \cdot 6H_2O$), hydrochloric acid (HCl), ammonium chloride (NH_4Cl)，Sulfuric acid (H_2SO_4)， were purchased from Kelong chemically (Chengdu, China). Polyvinyl alcohol (PVA, Mw = 67000), Polytetrafluoroethylene (PTFE, 60 wt% of solid content), Sodium nitrate ($NaNO_3$)，sodium nitrite ($NaNO_2$), sodium nitroferricyanide dihydrate ($C_5FeN_6Na_2O \cdot 2H_2O$), sodium salicylate ($C_7H_5NaO_3$), salicylic acid ($C_7H_6O_3$), trisodium citrate dihydrate ($C_6H_5Na_3O_7 \cdot 2H_2O$), sodium hypochlorite solution (NaClO), pp-dimethylamino benzaldehyde ($C_9H_{11}NO$), 0.8 wt% sulfamic acid solution (H_3NO_3S), were purchased from Aladdin Ltd (Shanghai, China). Nafion solution (5 wt%) was purchased from Sigma-Aldrich Chemical Reagent Co., and Ltd. Deionized water was purified through a Millipore system.

Preparation of catalysts: Co_3O_4@CNF was prepared by the electrospinning method. Firstly, 0.1 g of $Co(NO_3)_2 \cdot 6H_2O$, 1.5 g of PVA were dissolved in 10 mL of water under vigorous stirring at 90 °C for 180 min. 10 g of PTFE was then added into the solution. Subsequently, the prepared solution was moved to a syringe with a stainless-steel nozzle. A high-voltage of 22 kV was supplied and the distance between the needle tip and the rotating drum collector is 22 cm. After electrospinning, the as-spun fibres were collected and heat-treated at 280 °C for 2 h in air. Co@CNF was

formed by carbonized the fiber at 800 °C for 2 h in Ar atmosphere. Co_3O_4@CNF was synthesized by oxidizing the Co@CNF in air at 300 °C for 2 h. CNF was prepared under the same conditions with Co@CNF without adding $Co(NO_3)_2 \cdot 6H_2O$.

Working electrode preparation: 5 mg catalyst were grinded into powder and added into a mixed solution containing 655 μL ethanol, 325 μL deionized water and 20 μL of 5 wt% Nafion solution, followed by 60 min ultrasonic dispersion to form a homogeneous suspension. Then, 20 μL of such suspension was dropped on carbon paper (CP, $1 \times 1 cm^2$), and dried at ambient temperature.

Characterizations: XRD data were acquired by a LabX XRD-6100 X-ray diffractometer with a Cu Kα radiation (40 kV, 30 mA). SEM measurements were carried out on a Gemini SEM 300 scanning electron microscope (ZEISS, Germany) at an accelerating voltage of 5 kV. TEM image was obtained from a Titan G260-300 transmission electron microscope operated at 200 kV. XPS measurements were performed on a Thermo Scientific K-Alpha photoelectron spectrometer. The absorbance data was collected on on SHIMADZU UV-1800 Ultraviolet-visible (UV-Vis) spectrophotometer. Gas was determined using Shimadzu gas chromatography (GC) (GC-2014). Ion chromatography data were acquired by ion chromatograph (Thermo Scientific ICS-900).

Electrochemical measurements: All electrochemical measurements were carried on the CHI660E electrochemical workstation (Shanghai, Chenhua) using a standard three-electrode setup. Electrolyte solution was Ar-saturated of 0.1 M NaOH with 0.1 M NO_3^-, using Co_3O_4@CNF (loading 0.1 mg) as working electrode, a Pt plate as the

counter electrode, and a Hg/HgO as the reference electrode. We use a H-type electrolytic cell separated by a Nafion 117 membrane which was protonated by boiling in ultrapure water, H_2O_2 (5%) aqueous solution and 0.5 M H_2SO_4 at 80 °C for another 2 h, respectively. All the potentials reported in our work were converted to reversible hydrogen electrode via calibration with the following equation: E (RHE) = E (Hg/HgO) + (0.098 + 0.0591 × pH) V.

Determination of NH_3: The NH_3 concentration in the electrolyte was determined by colorimetry using the indophenol blue method. The post-electrolytes using Co_3O_4@CNF as work electrode are diluted 40 times before testing. The post-electrolytes using Co@CNF as work electrode are diluted 10 times before testing. The post-electrolyte using CNF as work electrode − 0.9 V is only diluted 1 time before testing. In detail, 2 mL of the solution after reaction, and 2 mL of 1 M NaOH coloring solution containing 5% salicylic acid and 5% sodium citrate. Then, 1 mL oxidizing solution of 0.05 M NaClO and 0.2 mL catalyst solution of $C_5FeN_6Na_2O$ (1 wt%) were added to the above solution. After standing in the dark for 2 h, the UV-Vis absorption spectra were measured. The concentration of NH_3 was identified using the absorbance at a wavelength of 655 nm. The concentration-absorbance curve was calibrated using the standard NH_4Cl solution in 0.1 M NaOH solution. The fitting curve ($y = 0.51697x + 0.0365$, $R^2 = 0.999$) shows good linear relation of absorbance value with NH_3 concentration.

Detection of NO_2^-: The concentration of NO_2^- was quantificationally analyzed by the Griess method. The obtained electrolyte was diluted 10 times. Firstly, the coloring

reagent for NO_2^- was prepared as follow: 0.1 g of N-(1-naphthyl)-ethylenediamine dihydrochloride, 1.0 g of sulfonamide and 2.94 mL of H_3PO_4 were dissolved in 50 mL of deionized water. Next, 40 μL catholyte was diluted to 2 mL and 1 mL of diluted solution was mixed with 1 mL of coloring reagent and 2 mL of deionized water. After shaking and standing for 10 minutes, the UV-Vis spectrophotometry was used to measure the absorbance at a wavelength of 540 nm. The concentration of NO_2^- was calculated based on the calibration curve ($y = 0.22406x + 0.02224$, $R^2 = 0.999$).

Determination of N_2H_4: The Watt and Chrisp method are adopted to detect N_2H_4 in the electrolyte. In details, $C_9H_{11}NO$ (5.99 g), HCl (30 ml) and C_2H_5OH (300 mL) are mixed to form an uniform solution used as a color reagent. Then, 1 mL of color reagent is added into 1 mL of electrolyte after 1 h electrolysis. The absorbance is performed at a wavelength of 455 nm after the mixture stands 20 min in darkness. The fitting curve ($y = 0.3263x + 0.06524$, $R^2 = 0.998$) shows a good linear relation of absorbance value with N_2H_4 concentration.

Detection of H_2: In the NITRR process, there is a competitive reaction HER in cathode. H_2 can be detected by blowing the product after electrolysis in the cathode chamber into a gas chromatograph (GC). In order to reduce the experimental error caused by the different thermal conductivity of the gas, the carrier gas of the chromatography is nitrogen. Nitrogen is passed into the cathode electrolyte at a flowing rate of 20 mL min^{-1}, and GC collected the gas produced by the reaction in the cathode chamber every 5 minutes. The hydrogen concentration can be obtained by integrating the characteristic peaks of hydrogen collected in the TCD detector.

Calculations of the FE and NH_3 yield rate:

FE toward NH_3 via NITRR was calculated by the following equation:

$$FE = (8 \times F \times [NH_3] \times V) / (17 \times Q) \times 100\%$$

NH_3 yield rate is calculated using the following equation:

$$NH_3 \text{ yield} = ([NH_3] \times V) / (t \times m_{cat.})$$

Where F is the Faradaic constant (96480 C mol^{-1}), $[NH_3]$ is the measured NH_3 concentration, V is the volume of electrolyte in the cathode compartment (40 mL), 17 is the molar mass of NH_3, Q is the total quantity of applied electricity; t is the electrolysis time and $m_{cat.}$ is the mass of catalyst (0.1 mg).

DFT calculation details:

First-principles calculations were performed within the density functional theory framework.[1] The projector-augmented wave (PAW) method [2, 3] and the generalized gradient approximation (GGA) [4] for the exchange-correlation energy functional, as implemented in the Vienna ab initio simulation package (VASP) [5-8] were used. The GGA calculation was performed with the Perdew-Burke-Ernzerhof (PBE) [9] exchange-correlation potential. Considered long-range interaction between molecules/intermediates and surface, Van der Waals interactions were considered using DFT-D3 correlation.[10] The convergence criterion of geometry relaxation was set to 0.03 eV·$Å^{-1}$ in force on each atom. The energy cutoff for plane wave-basis was set to 600 eV. The K points were sampled with 3×3×1, 3×3×1, and 3×3×3 by Monkhorst-Pack method for Co (111), Co_3O_4 (311), and Co_3O_4 cluster, respectively.

The change in free energy (ΔG) of per reaction step was calculated as following:[11]

$$\Delta G = \Delta E + \Delta ZPE - T \cdot \Delta S + \Delta G_U + \Delta G_{pH}$$

Where ΔE is the change of the total reaction energy obtained from DFT calculation, ΔZPE is the change of the zero-point energy, T is the temperature (300K), and ΔS is the change of the entropy. $\Delta G_U = -eU$, where U is the potential at the electrode and e is the transferred charge. $\Delta G_{pH} = k_B \cdot T \times \ln 10 \times pH$, where k_B is the Boltzmann constant and T = 300 K. In this work, the influence of pH was neglected.

For HER, the hydrogen adsorption energy (ΔE_{H*}) was calculated by the following equation:[12]

$$\Delta E_{H^*} = E_{H^*} - (E_* + 1/2E_{H_2})$$

Where E_{H^*} is the total energy of H atom on the support, E_* is the total energy of support, E_{H_2} is the energy of the gas H_2 calculated by setting the isolated H_2 in a box of 10.0 Å×10.0 Å×10.0 Å. The Gibbs free energy for the well-known highly efficient Pt catalyst is near-zero as $|\Delta G_{ads}| \approx 0.09$ eV.[13]

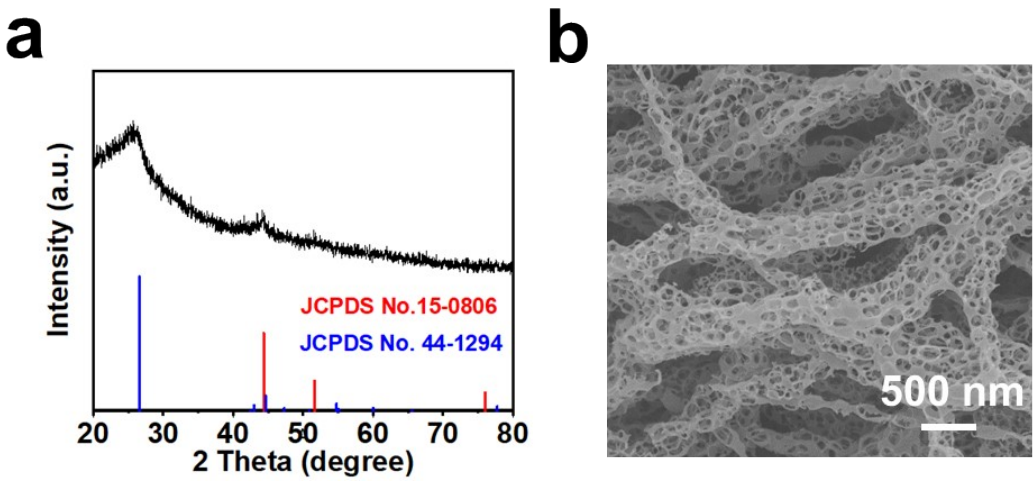

Fig. S1 (a) XRD pattern and (b) SEM image of Co@CNF.

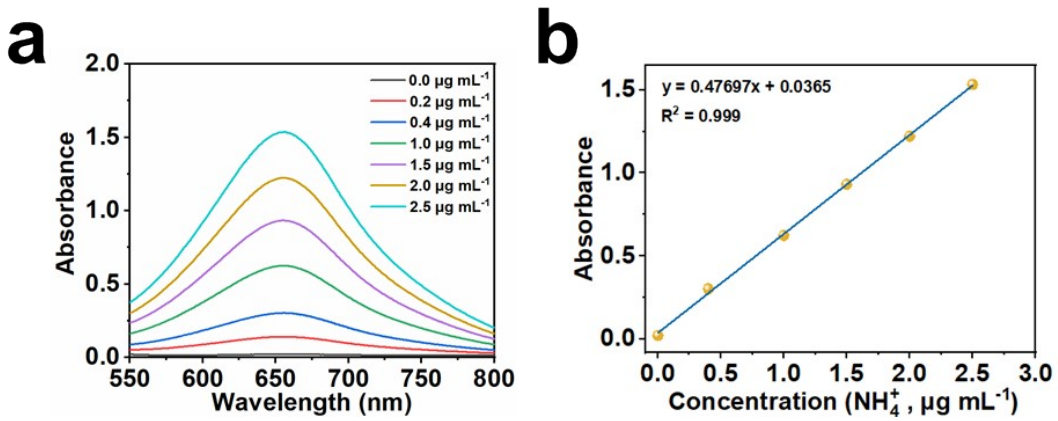

Fig. S2 (a) UV-Vis absorption spectra and (b) corresponding calibration curve of NH_4^+.

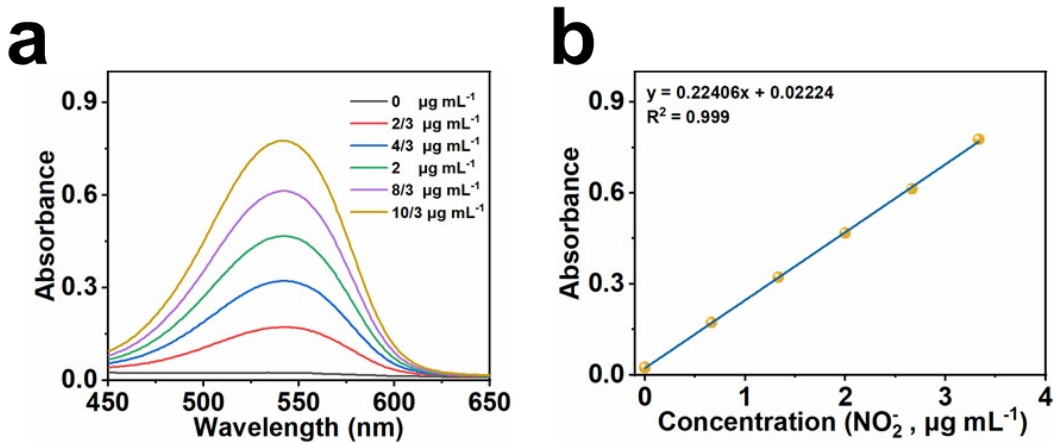

Fig. S3 (a) UV-Vis absorption spectra and (b) corresponding calibration curve of NO_2^-.

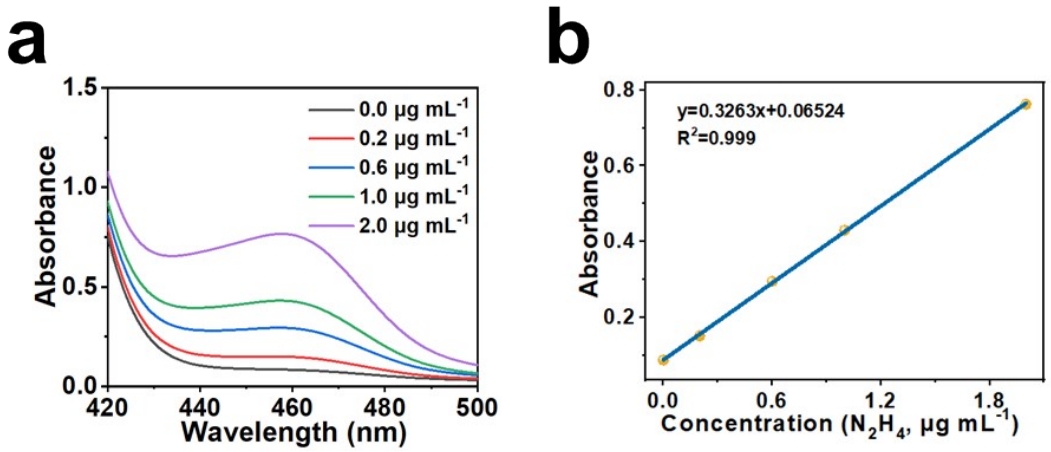

Fig. S4 (a) UV-Vis absorption spectra and (b) corresponding calibration curve of N_2H_4.

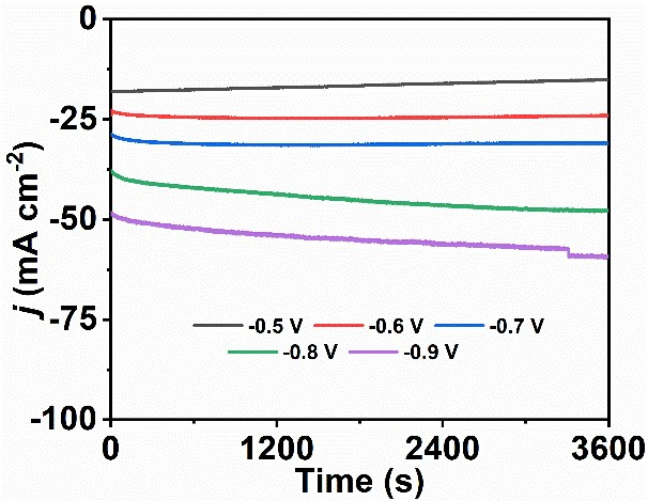

Fig. S5 CA curves in 0.1 M NaOH solution with 0.1 M NO_3^- at different applied potentials for 1 hour.

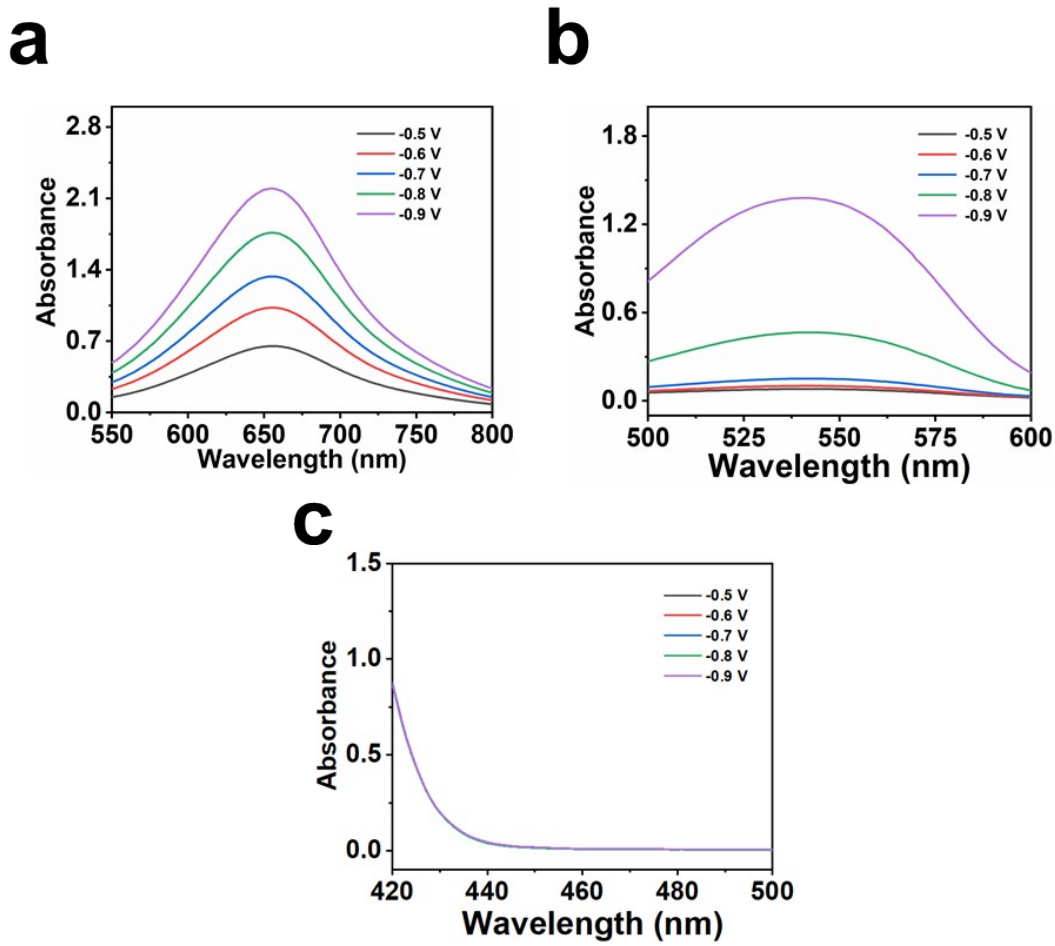

Fig. S6 UV-Vis spectra of (a) NH_3, (b) NO_2^- and (c) N_2H_4 on Co_3O_4@CNF electrode after 1 h electrolysis at different potentials.

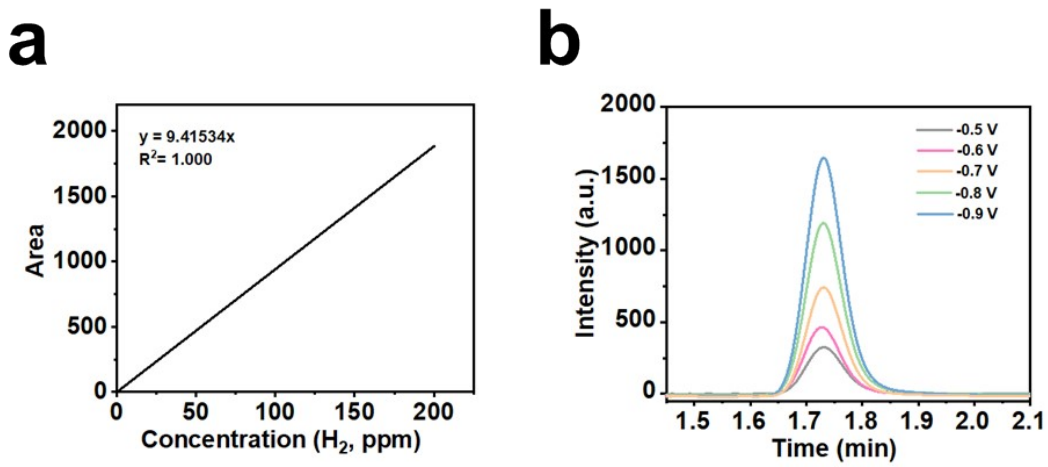

Fig. S7 (a) The standard curve for calculating the H_2 yield. (b) Signal intensity of H_2 detected by gas chromatography.

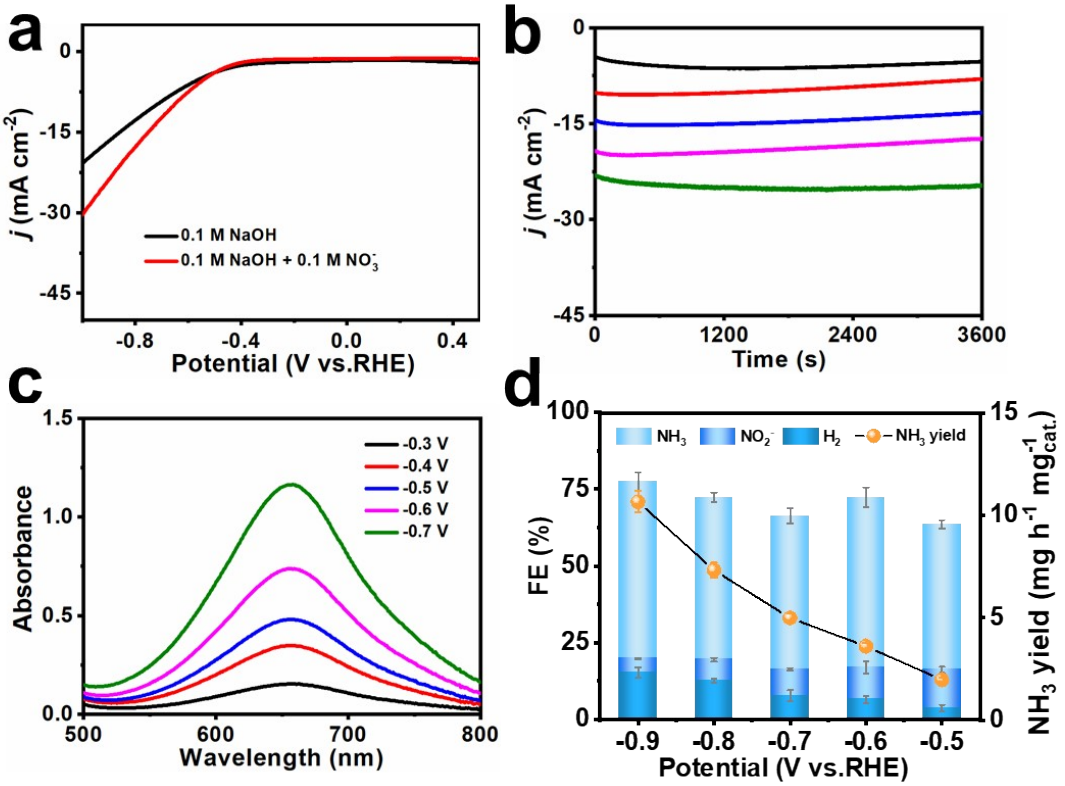

Fig. S8 (a) LSV curves of Co@CNF in 0.1 M NaOH solution with and without NO_3^-. (b) CA curves in 0.1 M NaOH solution with 0.1 M NO_3^- at different applied potentials for 1 hour. (c) UV-Vis spectra of NH_3 at different post-electrolysis electrolytes. (d) FEs of three reduction products and NH_3 yields of Co@CNF at different potentials.

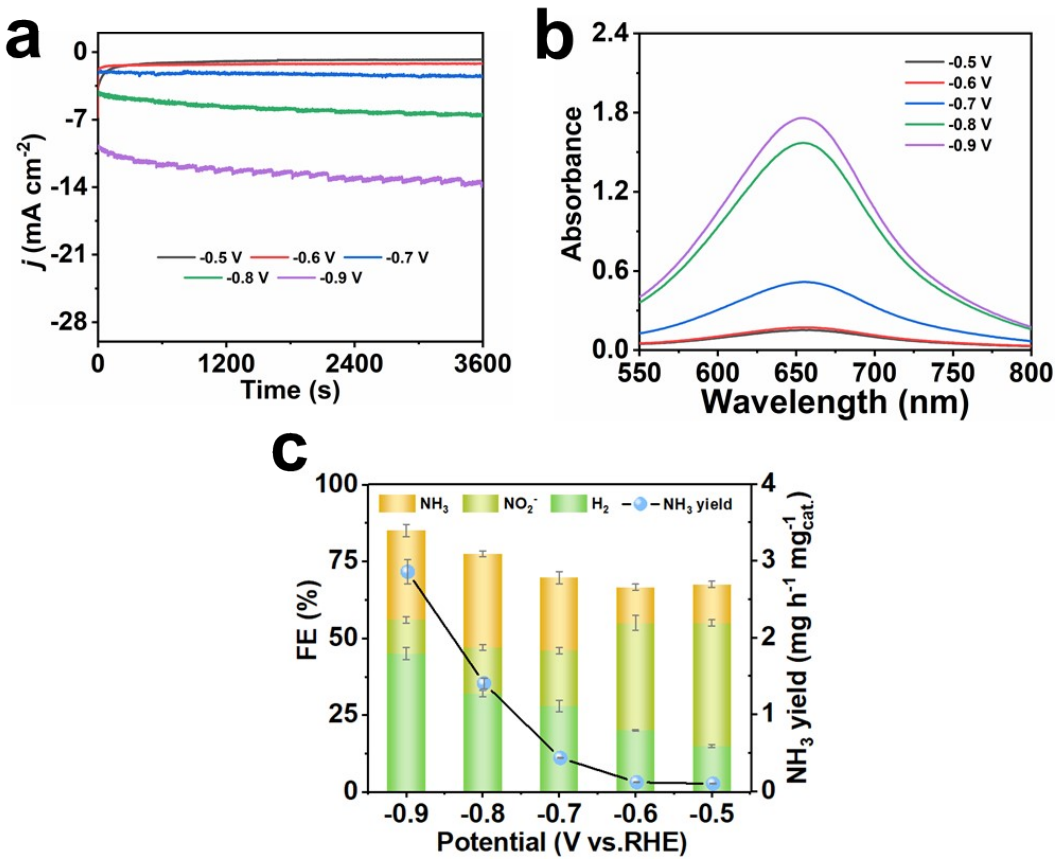

Fig. S9 (a) CA curves in 0.1 M NaOH solution with 0.1 M NO_3^- at different applied potentials for 1 hour. (b) UV-Vis spectra of NH_3 at different post-electrolysis electrolytes. (c) FEs of three reduction products and NH_3 yields at different potentials.

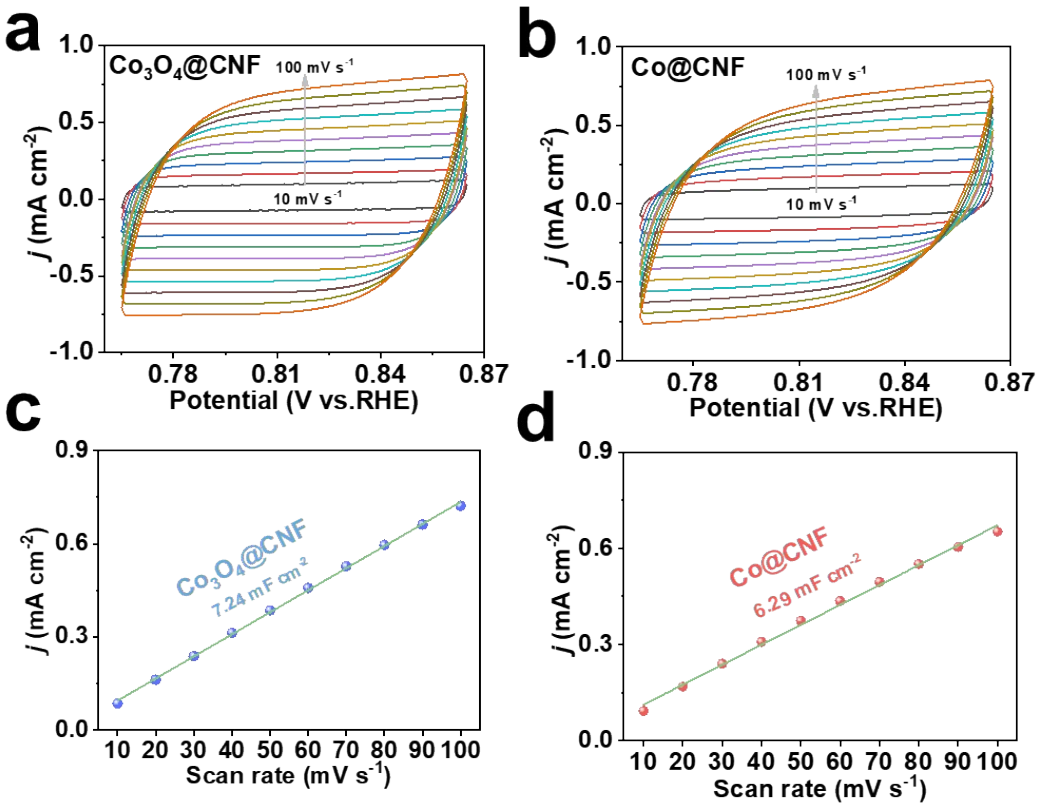

Fig. S10 CV curves of (a) Co_3O_4@CNF, (b) Co@CNF with different scan rates from 10 to 100 mV s^{-1}. Calculated double-layer capacitance of (c) Co_3O_4@CNF and (d) Co@CNF.

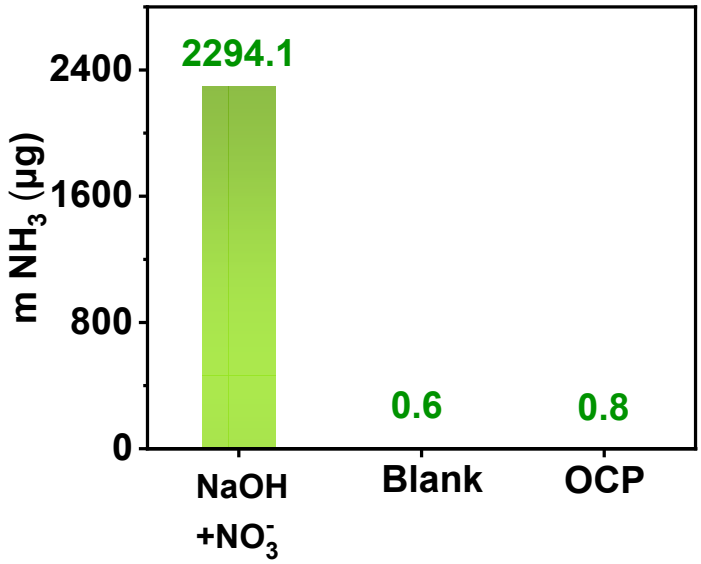

Fig. S11 NH_3 yields of electrolysis at −0.7 V in 0.1 M NaOH with 0.1 M NO_3^-, blank pre-electrolysis electrolyte and electrolysis at open-circuit potential for 1 hour.

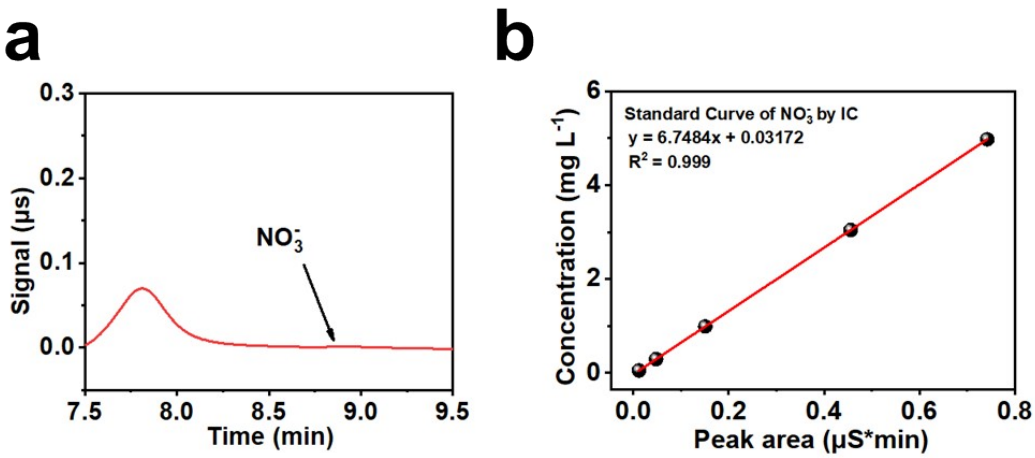

Fig. S12 (a) NO_3^- concentration in 0.1 M NaOH detected by IC. (b) The standard curve of NO_3^-.

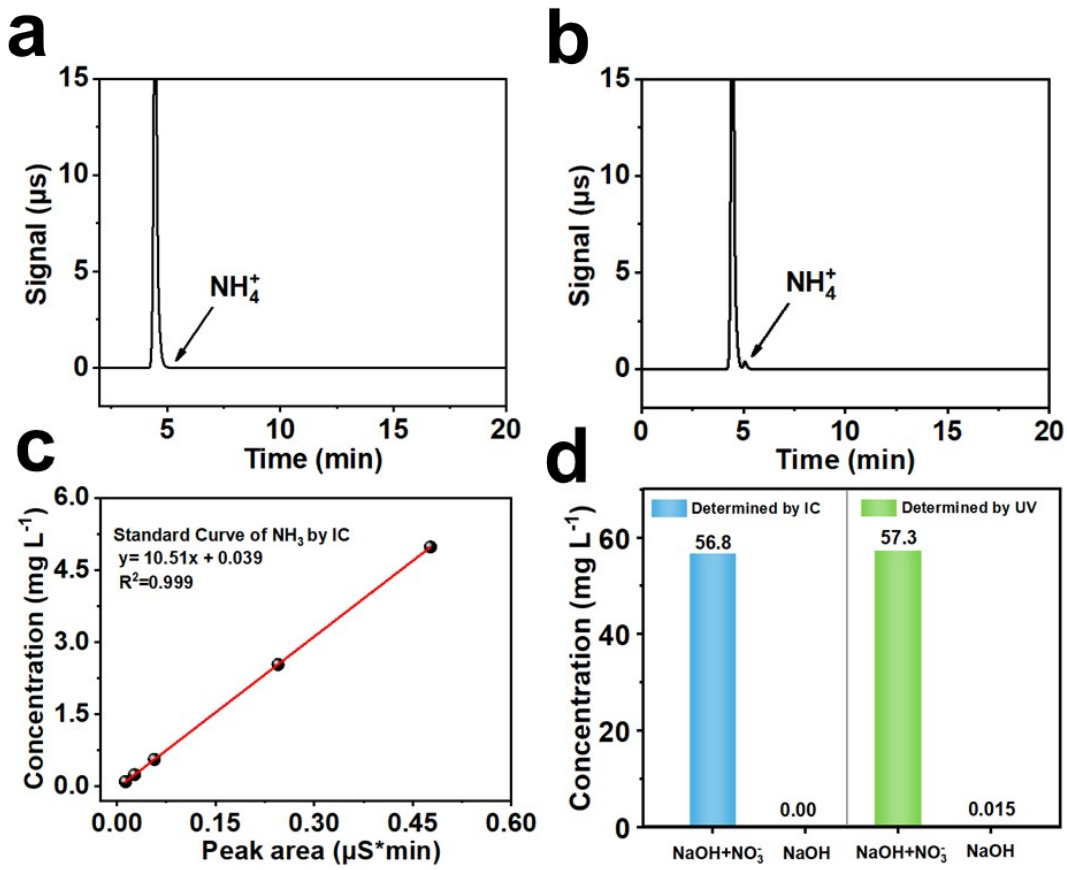

Fig. S13 (a) IC curve of Co_3O_4@CNF in 0.1 N NaOH. (b) IC curve of Co_3O_4@CNF in 0.1 N NaOH with 0.1 M $NaNO_3$. (c) The standard curve for calculating the NH_3 yield by IC. (d) NH_3 yield detected by UV-Vis spectroscopy and IC.

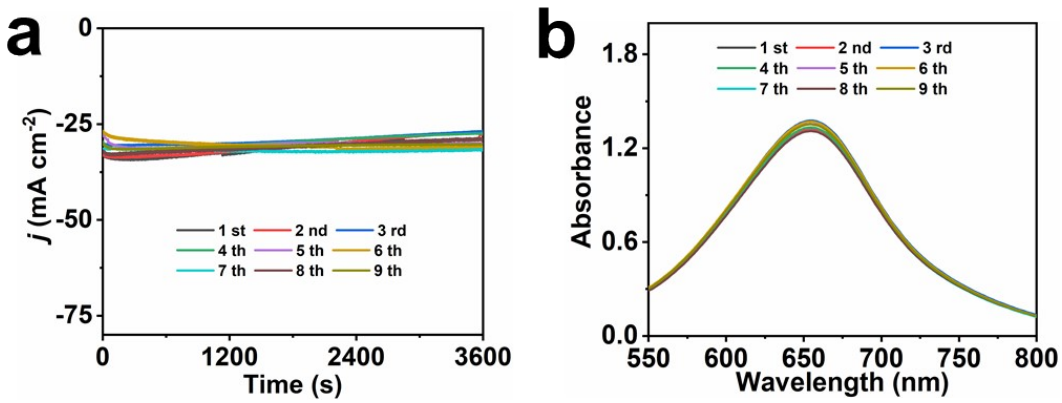

Fig. S14 (a) CA curves in 0.1 M NaOH with 0.1 M NO_3^- and (b) UV–Vis spectra of recycling test at −0.7 V.

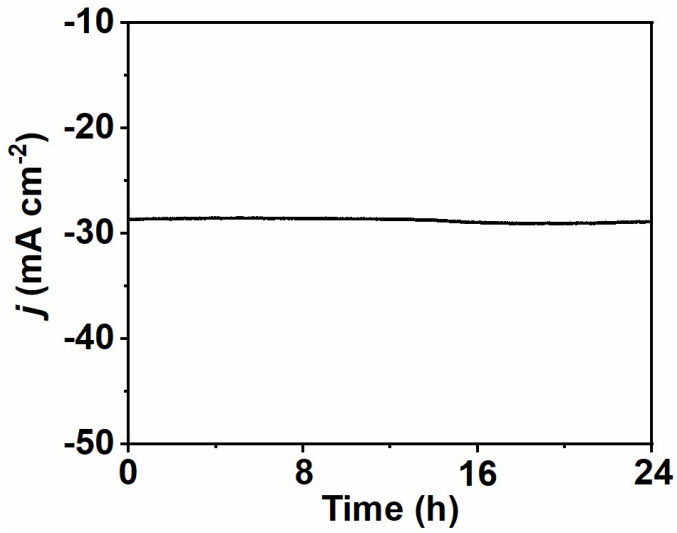

Fig. S15 CA curve of 24 h electrolysis in 0.1 M NaOH with 0.1 M NO_3^- on Co_3O_4@CNF electrode.

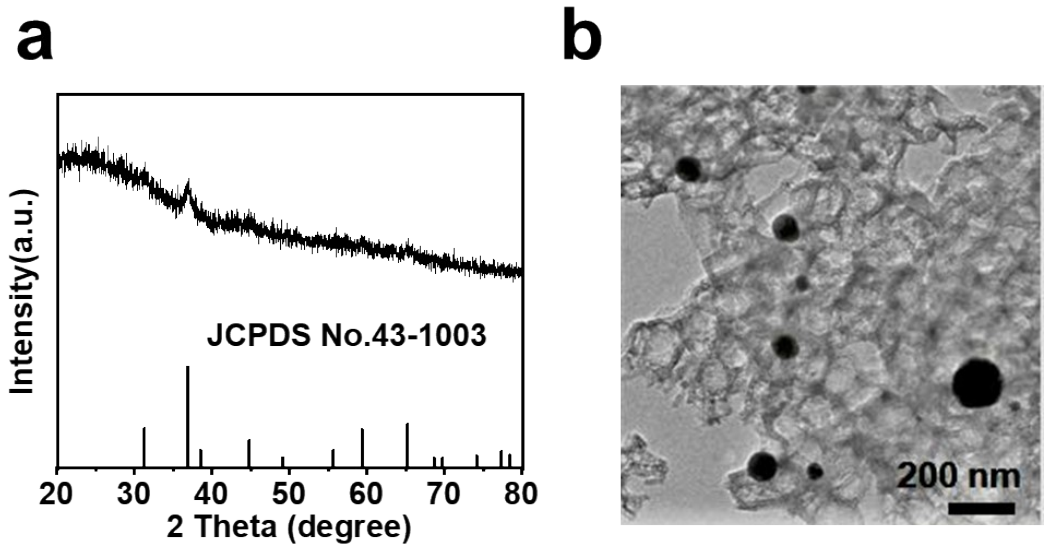

Fig. S16 The XRD pattern and TEM image of Co_3O_4@CNF after testing.

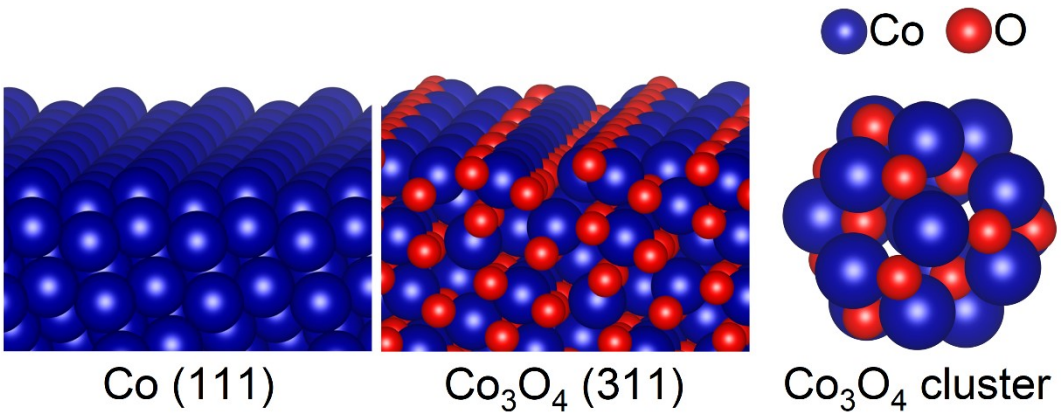

Fig. S17 The calculated models of Co (111), Co_3O_4 (311) and Co_3O_4 cluster.

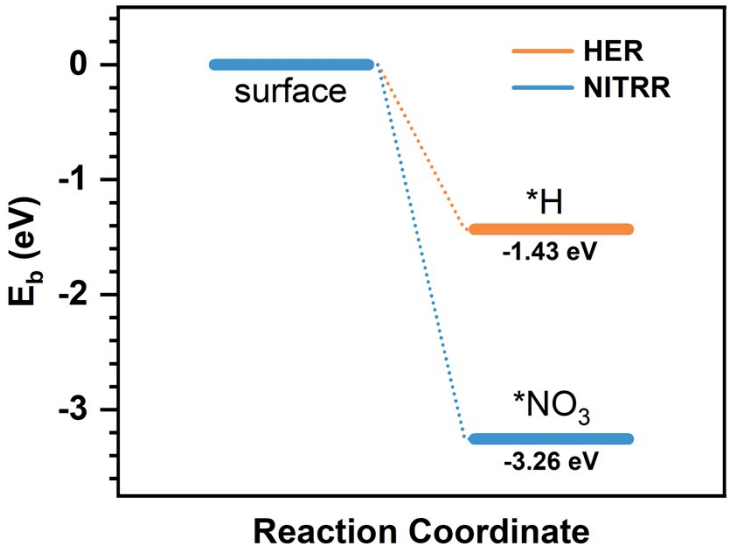

Fig. S18 The calculated E_b of proton (*H) and NO_3^- group (*NO_3).

Table S1 Comparison of performance for Co_3O_4@CNF with other reported NO_3RR electrocatalysts.

Catalysts	potential (V vs. RHE)	NH_3 yield ($mg\ h^{-1}mg^{-1}_{cat.}$)	FE (%)	Electrolyte	Ref.
Co_3O_4 @CNF	**−0.7**	**20.36**	**94.4**	**0.1 M PBS + 0.1 M $NaNO_3$**	**This work**
Cu (111) nanodisks	−0.63	2.16	81.11	0.1 M KOH + 0.01 M KNO_3	14
PdNi nanosheets	−1.2	16.7	87.9	0.5 M Na_2SO_4 + 0.1 M $NaNO_3$	15
Ni_3N/N-C-800 nanohybrids	−1.45	11.71	85.0	0.5 M Na_2SO_4 + 0.05 M $NaNO_3$	16
Pd nanodots on Zr-MOF	−1.3	0.287	58.1	0.1 M Na_2SO_4 + 500 ppm $NaNO_3$	17
In–S–G	−0.7	3.74	75.0	0.1 M KOH + 0.1 M KNO_3	18
Fe single-atom catalysts	-0.66	20	76.0	0.1M K_2SO_4 + 0.5 M KNO_3	19
Cu-N_4	-0.89	0.274	82.1	0.2 M Na_2SO_4 + 0.2 M $NaNO_3$	20
Cu–Pd/C nanobelts	-0.4	0.221	62.3	0.1 M KOH + 0.01 M KNO_3	21
PP-Co/CP	-0.7	18.7	90.1	0.1 M NaOH + 0.1 M $NaNO_3$	22
Cu@ZrO_2	-0.7	15.4	67.6	0.1 M PBS + 0.1 M $NaNO_3$	23

Reference

1. W. Kohn and L. J. Sham, *Phys. Rev.*, 1965, **140**, A1133-1138.
2. P. E. Blöchl, *Phys. Rev. B*, 1994, **50**, 17953.
3. G. Kresse and D. Joubert, *Phys. Rev. B*, 1999, **59**, 1758-1775.
4. J. P. Perdew and Y. Wang, *Phys. Rev. B*, 1992, **45**, 13244-13249.
5. G. Kresse and J. Hafner, *Phys. Rev. B*, 1993, **47**, 558-561.
6. G. Kresse and J. Furthmüller, *Phys. Rev. B*, 1996, **54**, 11169.
7. L. Chen, L. Z. Zhou, H. B. Lu, Y. Q. Zhou, J. L. Huang, J. Wang, Y. Wang, X. L. Yuan and Y. Yao, *Chem. Commun.*, 2020, **56**, 9138-9141.
8. G. Kresse and J. Furthmüller, *Comput. Mater. Sci.*, 1996, **6**, 15-50.
9. J. P. Perdew, K. Burke and M. Ernzerhof, *Phys. Rev. Lett.*, 1996, **77**, 3865-3868.
10. S. Grimme, J. Antony, S. Ehrlich and H. Krieg, *J. Chem. Phys.*, 2010, **132**, 154104.
11. J. K. Nørskov, J. Rossmeisl, A. Logadottir, L. Lindqvist, J. R. Kitchin, T. Bligaard and H. Jonsson, *J. Phys. Chem. B*, 2004, **108**, 17886-17892.
12. Y. Zheng, Y. Jiao, Y. H. Zhu, L. H. Li, Y. Han, Y. Chen, A. J. Du, M. Jaroniec and S. Z. Qiao, *Nat. Commun.*, 2014, **5**, 1-8.
13. J. K. Nørskov, T. Bligaard, A. Logadottir, J. Kitchin, J. G. Chen, S. Pandelov and U. Stimming, *J. Electrochem. Soc.*, 2005, **152**, J23-J26.
14. K. Wu, C. Sun, Z. Wang, Q. Song, X. Bai, X. Yu, Q. Li, Z. Wang, H. Zhang and J. Zhang, *ACS Mater. Lett.*, 2022, **4**, 650-656.
15. G. Zhang, X. Li, P. Shen, Y. Luo, X. Li and K. Chu, *J. Environ. Chem. Eng.*, 2022, **10**, 108362.

16. X. Zhang, G. Ma, L. Shui, G. Zhou and X. Wang, *Chem. Eng. J.*, 2022, **430**, 132666.

17. M. Jiang, J. Su, X. Song, P. Zhang, M. Zhu, L. Qin, Z. Tie, J.-L. Zuo and Z. Jin, *Nano Lett.*, 2022, **22**, 2529-2537.

18. F. Lei, W. Xu, J. Yu, K. Li, J. Xie, P. Hao, G. Cui and B. Tang, *Chem. Eng. J.*, 2021, **426**, 131317.

19. Z.-Y. Wu, M. Karamad, X. Yong, Q. Huang, D. A. Cullen, P. Zhu, C. Xia, Q. Xiao, M. Shakouri and F.-Y. Chen, *Nat. Commun.*, 2021, **12**, 2870.

20. J. Cheng, W. Sun, G. Dai, X. Yang, R. Xia, Y. Xu, X. Yang and W. Tu, *Fuel*, 2023, **332**, 126106.

21. Z. Wang, C. Sun, X. Bai, Z. Wang, X. Yu, X. Tong, Z. Wang, H. Zhang, H. Pang and L. Zhou, *ACS Appl. Mater. Interfaces*, 2022, **14**, 30969-30978.

22. Q. Chen, J. Liang, Q. Liu, K. Dong, L. Yue, P. Wei, Y. Luo, Q. Liu, N. Li and B. Tang, *Chem. Comm.*, 2022, **58**, 4259-4262.

23. J. Xia, H. Du, S. Dong, Y. Luo, Q. Liu, J. S. Chen, H. Guo and T. Li, *Chem. Comm.*, 2022, **58**, 13811-13814.